Combined Manuscript File

# The enigma of the respiratory chain supercomplex

Dusanka Milenkovic[1*], James N Blaza[2*], Nils-Göran Larsson[1,3,§] and Judy Hirst[2,§]

[1]Department of Mitochondrial Biology, Max Planck Institute for Biology of Ageing, Joseph-Stelzmann-Strasse 9b, 50931 Cologne, Germany; [2]Medical Research Council Mitochondrial Biology Unit, Cambridge CB2 0XY, United Kingdom; [3]Department of Medical Biochemistry and Biophysics, Karolinska Institutet, 171 77 Stockholm, Sweden.

* Co-first author

§ Correspondence to:

Nils-Göran Larsson or Judy Hirst

nils-goran.larsson@ki.se, jh@mrc-mbu.cam.ac.uk

**SUMMARY**

Respiratory chain dysfunction plays an important role in human disease and aging. It is now well established that the individual respiratory complexes can be organized into supercomplexes, and structures for these macromolecular assemblies, determined by electron cryo-microscopy, have been described recently. Nevertheless, the reason why supercomplexes exist remains an enigma. The widely-held view that they enhance catalysis by channeling substrates is challenged by both structural and biophysical information. Here, we evaluate and discuss data and hypotheses on the structures, roles and assembly of respiratory-chain supercomplexes, and propose a future research agenda to address unanswered questions.

## INTRODUCTION

The structure, function and organization of the respiratory chain have been under investigation since Otto Warburg discovered *Atmungsferment*, the enzymatic basis for cellular respiration (Warburg, 1928). Thirty years later, progress in understanding how the mitochondrial respiratory chain drives ATP synthesis culminated in Peter Mitchell's chemiosmotic hypothesis (Ernster and Schatz, 1981; Mitchell, 1961). Since then, molecular-level knowledge of the structures and mechanisms of the enzymes that comprise the respiratory chain and catalyze oxidative phosphorylation has exploded (Nicholls and Ferguson, 2013). Three proton-translocating complexes, complex I (CI, NADH:ubiquinone oxidoreductase), complex III (CIII, ubiquinol-cytochrome *c* oxidoreductase) and complex IV (CIV, cytochrome *c* oxidase), connected by the mobile electron carriers ubiquinone (Q, ubiquinone-10 in humans) and cytochrome *c* (cyt *c*), catalyze electron transfer from NADH to $O_2$. Many other pathways also contain enzymes that reduce ubiquinone to ubiquinol and so feed electrons into the respiratory chain. Proton translocation by CI, CIII and CIV generates a proton-motive force across the inner membrane that is used by $F_1F_o$-ATP synthase to synthesize ATP. Consistent with the central role of oxidative phosphorylation in cellular energy metabolism, deficiencies in the enzymes that catalyze it are important contributors to human disease, both to rare inherited conditions and common age-associated diseases (Picard et al., 2016).

The organization of the mitochondrial respiratory complexes is commonly discussed in terms of two extreme models, the 'fluid state' and 'solid state' models. In the solid state model the complexes that catalyze individual reactions associate into single units capable of catalyzing whole reaction pathways (Keilin and Hartree, 1947). These solid-state devices contain Q and cyt *c* to transfer electrons along pre-defined, enclosed pathways between their component complexes, and do not exchange them with the outside. In contrast, in the fluid model individual complexes diffuse freely in the membrane, and Q and cyt *c* move randomly and without restraint between them (Hackenbrock et al., 1986). The fluid model was generally accepted until the invention of blue native polyacrylamide gel electrophoresis (BN-PAGE). By preserving interactions between the complexes, this technique enabled the separation and visualization of the multi-enzyme assemblies now known as supercomplexes (Schägger and Pfeiffer, 2000). Supercomplexes were criticized initially as artifacts of mild detergent solubilization, but their existence was then supported by experiments using a variety of non-ionic detergents, and using separation by ultracentrifugation on sucrose density gradients (Acín-Pérez et al., 2008; Dudkina et al., 2005). Subsequently, they were observed in the absence of detergent in isolated cristae membranes, providing evidence of their existence *in*

*situ* (Davies et al., 2011). Supercomplexes have now been observed in diverse clades of organisms, including mammals (Schägger and Pfeiffer, 2000; 2001), plants (Eubel et al., 2003), yeast (Schägger and Pfeiffer, 2000), and some bacteria such as *Paracoccus denitrificans* (Stroh et al., 2004), a relative of the protomitochondrion. However, they are not universal. For example, *Escherichia coli* contains patches of identical complexes grouped together in different parts of its cell membrane (Llorente-Garcia et al., 2014). In mitochondria from mammalian tissues, BN-PAGE has revealed supercomplexes of varying stoichiometry including $CI/CIII_2/CIV_{1-4}$, $CI/CIII_2$ and $CIII_2/CIV_{1-2}$, and it has been estimated that 85-100% of CI and 55-65% of CIII, but only 15-25% of CIV, are found in supercomplexes (Greggio et al., 2016; Schägger and Pfeiffer, 2001). Respirasomes are supercomplexes that contain CI, CIII and CIV and are capable of $NADH:O_2$ oxidoreduction *in vitro* ($CI/CIII_2/CIV$ has been the most extensively studied). In organisms such as *Saccharomyces cerevisiae,* which do not express CI, only simpler superassemblies of CIII and CIV are present ($III_2/IV$ and $III_2/IV_2$) (Heinemeyer et al., 2007; Mileykovskaya et al., 2012; Schägger and Pfeiffer, 2000).

Here, we discuss how and why respiratory complexes are organized into supercomplex assemblies. Supercomplexes are now widely accepted by the scientific community, but the reason(s) for their existence, and whether they confer any functional or structural advantage, or contribute to the pathophysiology of human disease, remain under debate. We explore knowledge of their structures, evidence for specific factors that promote them, functional data on their proposed roles in enhancing catalytic efficiency or decreasing oxidative stress, and data relevant to the interplay between supercomplex formation and the topology, packing and stability of inner membrane structures.

**Structures of mammalian supercomplex assemblies**

Recent developments in single-particle electron cryo-microscopy (cryo-EM) (Fernandez-Leiro and Scheres, 2016) have led to a proliferation of relatively high resolution structural models of the mammalian respirasome (Gu et al., 2016; Letts et al., 2016; Sousa et al., 2016; Wu et al., 2016). Figures 1A and 1B show the structure of the respirasome from porcine heart mitochondria determined at 5.4 Å resolution (Gu et al., 2016). In the architecture shown, representative of all the mammalian structures described so far (Althoff et al., 2011; Dudkina et al., 2011; Gu et al., 2016; Letts et al., 2016; Sousa et al., 2016; Wu et al., 2016), the membrane arm of CI curves around the CIII dimer with CIV positioned on the toe of CI, interacting with both CI and CIII.

The structure of the porcine respirasome was published back-to-back with three

structures from ovine heart mitochondria (Letts et al., 2016), which arose from using cryo-EM particle classification to distinguish molecules with different compositions or conformations (Scheres, 2016). Two structures are respirasome structures, and one lacks CIV. Figure 1C compares the three respirasome structures (Gu et al., 2016; Letts et al., 2016) and highlights the conserved arrangement of CI and CIII but the varying location of CIV. From the porcine structure, to the 'tight' ovine respirasome, to the 'loose' ovine respirasome, and finally to the ovine structure lacking CIV entirely, CIV rolls around the tip of CI, gradually dissociating from CIII, and finally from the respirasome completely. Further structural variation has since been observed in data on the bovine respirasome, in which one class shows the CIII dimer rotated by 25º relative to CI (breaking specific interactions between them) (Sousa et al., 2016), and in further analyses of the porcine complex (Wu et al., 2016).

Figure 1C may depict the respirasome in various stages of disassembly, following its extraction from the membrane. Alternatively, respirasomes in the membrane may vary in structure, or be constantly dissociating, reforming and reorganizing. Tomographic structures of the complexes *in situ* (Davies et al., 2011; Wan and Briggs, 2016) and single molecule imaging (Wilkens et al., 2013) will be required to distinguish these alternatives. Importantly, the integrities of supercomplex assemblies in BN-PAGE are well known to depend on the type and concentration of detergent used to solubilize them out of the membrane; the solubilization condition must be strong enough to release the complexes, but mild enough to preserve the interactions between them. Furthermore, cryo-EM grid formation exposes samples to a large air-water interface and may destabilize or degrade weakly bound assemblies such as supercomplexes. Cryo-EM analyses themselves may provide additional bias by excluding large numbers of the particles imaged from the analysis. Whereas Sazanov and coworkers only discarded 22% of their imaged particles (Letts et al., 2016), Wang and coworkers discarded 62-64% (Gu et al., 2016; Wu et al., 2016) and Kühlbrandt and coworkers 75% (Sousa et al., 2016). Different approaches to particle classification and selection affect these values, but the substantial inhomogeneity present in all the preparations imaged deserves consideration.

The recent structures (Gu et al., 2016; Letts et al., 2016; Wu et al., 2016) have provided new information about specific interactions between subunits of the different complexes. Complexes I and III interact predominantly in two regions: NDUFA11 and NDUFB4 on CI interact with UQCRQ on CIII, and NDUFB9 and NDUFB4 interact with UQCRC1 and UQCRFS1 (the Rieske protein) (Letts et al., 2016; Wu et al., 2016). Notably, the contacts are dominated by the CI supernumerary (accessory) subunits, which are crucial for assembly and function of human CI (Stroud et al., 2016), rather than by the core subunits (Fiedorczuk et al.,

2016; Zhu et al., 2016). Although it has been proposed that the supernumerary subunits have undergone selection during evolution to favor supercomplex-stabilizing interactions (Letts et al., 2016), an equally valid proposal is that selection has instead favored them forming cage-like structures that protect the catalytically-active core subunits of the complexes from too close, restrictive interactions. The interactions that the less-tightly bound CIV forms with CI and CIII vary between the different respirasome structures (Letts et al., 2016; Wu et al., 2016), with a close interaction between CIV subunit COX7A and CIII subunit UQCR11 in the porcine structure that is progressively lost in the two ovine structures (Figure 1C).

**Relationship between supercomplexes and inner membrane architecture**

Mitochondria have a distinctive morphology due to being bounded by both an encasing outer membrane and an invaginated inner membrane that forms in-folded protrusions known as cristae. Cristae are pinched off at their base by the mitochondrial contact site and cristae organizing (MICOS) complex (Milenkovic and Larsson, 2015; Pfanner et al., 2014) separating the inner boundary membrane (which is juxtaposed to the outer membrane) from the cristae membrane (which projects into the matrix). Supercomplexes are highly enriched in the cristae membrane (Appelhans et al., 2012; Busch et al., 2013; Gilkerson et al., 2003; Vogel et al., 2006; Wilkens et al., 2013). $F_1F_o$-ATP synthase dimers define the membrane topology by organizing into ribbon-like structures on the highly curved tips of the cristae (Davies et al., 2011; Strauss et al., 2008). In contrast, the respiratory complexes are present predominantly on the planar cristae surfaces (Davies et al., 2011; Vogel et al., 2006; Wilkens et al., 2013). Consistent with this, a striking feature of the respirasome is its disc-like structure (Gu et al., 2016; Letts et al., 2016). Cristae remodelling (which disrupts the membrane topology) has been observed to disrupt the supercomplexes in the cristae (Cogliati et al., 2013) and an interdependent relationship between topology and supercomplex stability has probably arisen through their co-evolution. Finally, the dimerization of isolated CIV by interactions involving subunit COX6A (Tsukihara et al., 1996) has been used to suggest that respirasomes may form dimers and higher-order oligomers such as respiratory strings (Dudkina et al., 2010) through dimerization of their CIV monomers, since COX6A faces outside. However, when two supercomplex structures are aligned onto the CIV dimer structure the resulting supercomplex dimer is V-shaped, not planar (Letts et al., 2016). The larger supercomplex formed by arranging two CI and two CIV molecules around a common CIII dimer, as tentatively observed by Wu and coworkers (Wu et al., 2016) is more likely to remain consistent with the planar cristae membrane environment.

**Importance of phospholipid interactions for supercomplex structure and function**

Cardiolipin is the signature phospholipid of mitochondria, present in high amounts in the inner mitochondrial membrane (Mileykovskaya and Dowhan, 2009; 2013) where it is generally considered to stabilize supercomplexes in both yeast and mammals (Figure 2). Budding yeast strains with defective cardiolipin synthesis contain unstable supercomplexes that have only been visualized using clear native-PAGE, a milder version of BN-PAGE (Pfeiffer et al., 2003; Zhang et al., 2005). In addition, supercomplexes between CIII and CIV can only be reconstituted in liposomes when cardiolipin is present (Bazán et al., 2013). In mammalian systems, fewer supercomplexes can be observed in mitochondria from patients with Barth syndrome (McKenzie et al., 2006) who carry an X-linked mutation in the taffazin protein that transfers acyl chains between lipids and is required for cardiolipin remodeling (Schlame and Greenberg, 2017). Furthermore, it has been proposed recently that, by sequestering cardiolipin, the supercomplexes protect it from phospholipases (Xu et al., 2016). Thus, in Barth syndrome, defective cardiolipin remodeling may lead to decreased supercomplex stability, then (in a vicious cycle) to further cardiolipin release and degradation, augmenting the original effect.

In supercomplex structures the complexes are only loosely associated with one another, with plenty of space to accommodate phospholipids between them. Although cardiolipin is considered to stabilize supercomplexes, phosphatidylethanolamine, another inner membrane phospholipid, has been reported to destabilize them (Böttinger et al., 2012). Thus, maintaining the correct balance of phospholipid species between the complexes may be important. A number of phospholipids were resolved in the structure of the porcine respirasome, but in positions that probably stabilize individual complexes, rather than interactions between them (Wu et al., 2016). Indeed, it is well established that cardiolipin is required for the stability of many membrane proteins, including the respiratory chain complexes (McKenzie et al., 2006; Mileykovskaya and Dowhan, 2009; 2013), making it difficult to distinguish its effects on individual complexes from its effects on supercomplexes as a whole.

**Are specific proteins required for supercomplex formation or stability?**

Three independent groups have reported that respiratory complex factors 1 and 2 (Rcf1 and Rcf2) are required for formation/stabilization of CIII/CIV supercomplexes in yeast (Chen et al., 2012; Strogolova et al., 2012; Vukotic et al., 2012), and similarly a mammalian ortholog of Rcf1, Hig2a, affects CIV-containing supercomplexes (Chen et al., 2012). However, Rcf1 and Rcf2 have also been reported to be required for CIV assembly (Vukotic et al., 2012), Higd1a

(another ortholog of Rcf1) has been shown to bind to mammalian CIV and increase its activity by causing structural changes around heme *a* (Hayashi et al., 2015), and knocking out Rcf1 and Rcf2 in yeast decreased CIV activity (Rydström Lundin et al., 2016). Therefore, the effects of these proteins on supercomplex formation/stabilization are probably indirect. Likewise, the cardiolipin-binding protein C11orf83, reported to stabilize CIII-containing supercomplexes (especially $III_2$/IV in mammalian cells), is also necessary for both an early stage of CIII assembly and cristae maintenance (Desmurs et al., 2015). Another cardiolipin-binding factor, stomatin-like protein 2, reported to affect supercomplex formation/stabilization in T-cells, is also involved in compartmentalizing cardiolipin in the inner membrane (Mitsopoulos et al., 2015). Finally, mice deficient in the co-chaperone MCJ/DnaJC15, which has known roles in protein transport and sensitivity to chemotherapeutic agents (Sinha et al., 2016), have been reported to have higher levels of supercomplexes in their mitochondria, and higher rates of respiration. Thus, MCJ/DnaJC15 has been proposed as a negative regulator of supercomplex formation/stability (Champagne et al., 2016; Hatle et al., 2013). However, rates of CI catalysis are increased in the deficient mice, and levels of monomeric CI are not appreciably decreased, suggesting the results are influenced by higher CI content and/or activity and that the effects of MCJ/DnaJC15 on supercomplex formation/stabilization may be indirect also.

No densities from any of these proteins have been identified in structural data (Gu et al., 2016; Letts et al., 2016; Wu et al., 2016). Although available cryo-EM density maps are not yet at high enough resolution to allow individual residues to be identified, and so have been modeled by docking in the pre-existing structures of each individual complex (Fiedorczuk et al., 2016; Iwata et al., 1998; Tsukihara et al., 1996; Vinothkumar et al., 2014; Zhu et al., 2016), all the protein densities observed are accounted for by the 80 subunits of CI, CIII and CIV. It cannot be excluded that additional features will be resolved at higher resolution, but it is to be expected that transmembrane helix-containing proteins with important stabilizing roles would already have been observed because such proteins are expected to be tightly and stoichiometrically bound between the complexes. Although no supercomplex assembly factors have been identified in structural data, the existence of such factors cannot be excluded because they would be expected to only associate transiently with the nascent supercomplex.

In contrast to the proteins described above, the COX7A2-like protein COX7A2L (a.k.a. supercomplex assembly factor 1 or SCAFI), was described as a specific factor required for the interaction between CIII and CIV and thus for formation/stabilization of the $III_2$/IV and I/$III_2$/IV (respirasome) supercomplexes (Ikeda et al., 2013; Lapuente-Brun et al., 2013). The report that C57BL/6 mice harbor a shorter allele of *Cox7a2l*, which leads to the expression of

an unstable COX7A2L protein and lack of CIV-containing supercomplexes (Lapuente-Brun et al., 2013), contrasted with previous observations of respirasomes in C57BL/6 mice (Milenkovic et al., 2013; Sterky et al., 2012). In a study directly comparing mouse strains expressing the short (C57BL/6J, C57BL/6N) and long isoforms of *Cox7a2l* (CD1, BALB/c), it was confirmed that the $III_2$/IV supercomplex is dependent on the long isoform of COX7A2L (Mourier et al., 2014). However, fully assembled respirasomes and normal respiratory chain function were clearly observed in mice expressing both isoforms (Mourier et al., 2014). A mouse knockout for *Cox7a2l* created on the C57BL/6 background also showed the presence of CIV-containing supercomplexes, although their steady-state levels appeared lower (Ikeda et al., 2013), and studies in human cell lines found respirasome formation to be independent of the presence of COX7A2L (Pérez-Pérez et al., 2016). Enríquez and coworkers subsequently proposed that respirasomes are present in the heart and skeletal muscle of mice expressing the short COX7A2L isoform, but absent from the liver and most other tissues (Cogliati et al., 2016). However, other studies have observed respirasomes in the liver of mice expressing the short COX7A2L isoform (Jha et al., 2016; Mourier et al., 2014; Williams et al., 2016) (Table 1). Therefore, COX7A2L is not essential for formation/stabilization of the respirasome. It clearly does assist in formation/stabilization of the $III_2$/IV supercomplex (Pérez-Pérez et al., 2016), which can only been observed in mice that harbor the long COX7A2L isoform, and not in the C57BL/6 strain (Table 1 and Figure 2).

Due to lack of additional attributable density for COX7A2L in recent cryoEM maps, and high sequence similarity between COX7A2L and tissue-specific isoforms of COX7A, it was speculated that COX7A2L may replace COX7A in supercomplexes, acting as a bridge between CIII and CIV and stabilizing the $III_2$/IV interaction (Letts et al., 2016). Figure 1C shows how COX7A/COX7A2L moves relative to CIII subunit UQCR11 in the three respirasome structures described, consistent with the CIII/CIV interface being an inherently weak point of the respirasome and with COX7A/COX7A2L being a central feature of this interface. In mass spectrometric analyses of digitonin-solubilized mitochondria from CD1 mice (that express the long COX7A2L isoform), COX7A was present almost exclusively in monomeric/dimeric CIV, whereas COX7A2L was present in $III_2$/IV supercomplexes and respirasomes (Cogliati et al., 2016). We have previously shown that COX7A2L is a CIII-associated protein (Pérez-Pérez et al., 2016), and Enríquez and coworkers also detected COX7A2L bound to CIII in C57BL/6 mice (Cogliati et al., 2016). Together, these observations suggest that the homologous region of COX7A2L substitutes for COX7A and interacts with CIV, and that CIII donates COX7A2L to form the $III_2$/IV interface. Figure 3 proposes how the

long COX7A2L isoform displaces COX7A from CIV to form a tight $III_2$/IV interface either in $III_2$/IV-containing supercomplexes or respirasomes. It also suggests how respirasomes with only a weak $III_2$/IV interface form in the absence of COX7A2L, through interactions solely with CI. Whether the variants of the respirasome structure shown in Figure 1C correspond to respirasomes with tight or weak $III_2$/IV interfaces formed in these ways is not known.

Enríquez and coworkers used mutagenesis to identify residues in mouse COX7A2L that are important for the $III_2$/IV interaction (Cogliati et al., 2016). They found that His73, within the COX7A homologous region, is critical for the interaction between COX7A2L and CIV. The microdeletion in the short COX7A2L isoform removes two amino acid residues adjacent to His73, which may explain its inability to promote the $III_2$/IV interaction (Cogliati et al., 2016). Intriguingly, His73 in COX7A2L and the corresponding histidines in COX7A1 and COX7A2 are all replaced by tyrosines in humans, further underlining the importance of conserving this residue. Moreover, the roles of COX7A1/A2 and COX6A1/A2, which are subunits of CIV with tissue specific expression, were investigated and it was proposed that COX7A1 and COX6A2 promote CIV dimerization (Cogliati et al., 2016).

**Interpreting supercomplex structures to learn about their functions**

It is not easy to derive information about the catalytic mechanisms of redox enzymes from their structures. For the respirasome it is striking that the same structural information has repeatedly been interpreted in two very different ways, to either support or dismiss substrate-channeling hypotheses. In 2011, Kühlbrandt and coworkers (Althoff et al., 2011) proposed that supercomplexes are solid-state devices that construct pathways for the enclosed exchange of ubiquinone/ubiquinol between CI and CIII, and for cyt *c* between CIII and CIV, and they repeated this assertion recently (Sousa et al., 2016). In contrast, also in 2011, Boekema and coworkers (Dudkina et al., 2011) noted that proximity of the active sites may help to decrease the time required for random diffusion between them, but considered the concept of constructing the supercomplex to decrease the distances questionable. In 2016, Sazanov and coworkers noted the distinct lack of any substrate channels, or barriers to free diffusion, to connect the substrate-binding sites of CI, CIII and CIV in their structures (Letts et al., 2016).

Figure 4A uses a structural perspective to consider the possibility that Q is channeled through the membrane, between CI and CIII. Ubiquinol exits CI at a peripheral location in the supercomplex (Baradaran et al., 2013; Zhu et al., 2016) and no confining structure exists to guide it to the $Q_o$ site of the closest CIII monomer, on the opposite face of the membrane. Thus, it is free to diffuse in and out of the region between the two binding sites and to

exchange with the greater membrane environment — the lack of confining structure is inconsistent with substrate channeling. The structures of enzymes that really do channel substrates (typically highly reactive or toxic substrates) exhibit enclosed channels between the sites, which allow no escape or exchange (Weeks et al., 2006). Similarly, Figure 4B considers the possibility of cyt *c* channeling between CIII and CIV. Cyt *c* is located in the intermembrane space and diffuses in a thin volume along the inner membrane surface (Gupte and Hackenbrock, 1988). In Figure 4B, two cyt *c* molecules have been added to indicate their relative size and approximate binding sites on CIII (Lange and Hunte, 2002). Reduced cyt *c* interacts with a negatively-charged patch on CIV (Shimada et al., 2016; Tsukihara et al., 1996). Again, no confining structures exist to contain the cyt *c* molecules between the two specific sites and prevent them diffusing away. Therefore, structural data do not support substrate channeling. The close proximities of the active sites within the supercomplex may increase the probability of a substrate re-reacting within the same respirasome, but the substrates are unconstrained and free to move in any direction, either within or between respirasomes. Indeed, the close active site proximities result naturally from the high packing density in the inner membrane, independently of the specific arrangements of the complexes in supercomplexes.

The orientation of the CIII dimer in the respirasome (one monomer facing CI and one facing out) has recently led to speculation that the 'inner' monomer may dominate catalysis because its ubiquinol-oxidizing $Q_o$ site is closest to the ubiquinol-producing site of CI (Sousa et al., 2016) and because the movement of its Rieske domain appears less hindered by CIV (Letts et al., 2016). The asymmetry imposed by the respirasome is not present in isolated CIII, in which both monomers are active (Sarewicz and Osyczka, 2015), so little data exists to address this hypothesis. Furthermore, despite decades of study and an extensive scientific literature, Yang and coworkers (Wu et al., 2016) used their structure to propose a new mechanism for CIII. Whereas ubiquinol is known to be oxidized at the $Q_o$ site on the inter-membrane space side of the membrane in a 'bifurcating' electron transfer reaction that, by sending one of the two electrons across the membrane to ubiquinone bound at the $Q_i$ site, increases the number of protons transported across the membrane (Sarewicz and Osyczka, 2015), Yang and coworkers proposed that ubiquinol is in fact oxidized at the $Q_i$ site, and that the two protons generated 'might' then be transported across the membrane (Wu et al., 2016). Their model is inconsistent with all extant data on the mechanism of CIII (Sarewicz and Osyczka, 2015) and with its known proton-pumping stoichiometry (Nicholls and Ferguson,

2013), and it fails to complete a basic Q cycle for proton-electron transfer across the membrane as embodied by Mitchell's chemiosmotic theory (Mitchell, 1975).

**Supercomplexes do not channel substrates or partition the Q or cyt *c* pools**

Early work on distinguishing whether the Q pool in the inner mitochondrial membrane behaves as a single, freely-diffusing homogenous pool or whether Q molecules are sequestered into individual solid-state supercomplexes, has been reviewed in detail previously (Rich, 1984). Several lines of evidence led to a general consensus for a single, homogeneous pool that exchanges between all the membrane-bound complexes: i) calculations based on the diffusion coefficient of Q estimated that around 80 CIII dimers could be visited during a single CIII turnover during state 3 respiration; ii) predictions based on pool equations and comparison with experimental data provided evidence for a common substrate pool that could be reduced either by CI or CII (Kröger and Klingenberg, 1966; 1973); and iii) extraction of quinones followed by their reconstitution into membranes (which were also diluted with additional lipids) revealed a dependence on Q concentration consistent with a mobile Q pool in stoichiometric excess over the enzyme complexes (Schneider et al., 1982; 1980).

The solid-state model was subsequently revived by identification of supercomplex assemblies by BN-PAGE, and particularly by a report stating that isolated respirasomes (excised from BN-PAGE gels) that contain CI, CIII and CIV as well as co-purified Q and cyt *c* are able to catalyze electron transfer from NADH to $O_2$ (Acín-Pérez et al., 2008). Indeed, the isolated respirasome can be considered a solid-state device (Q is trapped in its phospholipid/detergent micelle and cyt *c* remains associated) — but once it is placed in a membrane diffusion and exchange of Q and cyt *c* may occur. Data from flux control analyses have been taken to support the existence of independently-catalyzing respirasomes embedded in the membrane (Bianchi et al., 2004). In these analyses, a particular step in a pathway is inhibited and the effects on the isolated step and on the pathway compared. If the inhibition is identical, then the step has complete control over the pathway flux and its flux control coefficient (FCC) is 1. Lenaz and coworkers used rotenone and mucidin to obtain FCC values of 1 for both CI and CIII in the NADH oxidation pathway, suggesting they operate as a single entity (Bianchi et al., 2004). However, the analyses relied on large extrinsic concentrations of hydrophilic quinones and cyt *c* to assay the individual steps, whereas the pathway uses the Q and cyt *c* that exist *in situ*. Consequently, individual steps may behave differently in isolation and in the pathway, and high extrinsic quinone concentrations displace competitive inhibitors so the choice of inhibitor may affect the results. It has since been reported that two canonical

CI inhibitors, piericidin A and rotenone, give very different FCC values (Blaza et al., 2014): in different experimental systems, the values measured for piericidin A were between 0.2 and 0.7, but those for rotenone between 1.7 and 3.9. The sum of all the FCC values for a pathway should equal 1, so values greater than 1 are not biologically meaningful (Fell, 1992), and the inhibitor dependence of the FCC values further questions the reliability of this approach.

In 2013, Enríquez and coworkers re-proposed the solid model of the respiratory chain by reporting that supercomplexes define dedicated Q and cyt *c* pools (Lapuente-Brun et al., 2013). According to their model, neither Q nor cyt *c* form homogeneous pools, but instead each supercomplex contains its own tiny pools that do not exchange with the tiny pools in other supercomplexes. However, the data used to support this model are also consistent with other explanations that are dependent on neither the involvement of supercomplexes nor partitioning of the Q and cyt *c* pools. First, in mouse fibroblasts with a constitutively low CIII expression, the activity of CI was moderately decreased but the activity of CII slightly increased. Both observations were explained subsequently by the same authors by increased production of reactive oxygen species (ROS) leading to CI disassembly (Diaz et al., 2012) and to activation of CII by phosphorylation (Acín-Pérez et al., 2014). Second, in the same fibroblasts the rate of CI+CIII catalysis was unchanged but the rate of CII+CIII catalysis was decreased, and this interesting discrepancy led to the proposal that CI sequesters CIII into supercomplexes, leaving little CIII available for CII catalysis. However, an alternate and perhaps simpler explanation is that CI+CIII catalysis is limited by one or more factors external to the respiratory chain (e.g. the upstream production of NADH) and therefore not affected by decreased CI or CIII activity, whereas CII+CIII catalysis is limited by CIII. Third, the authors observed that in CD1 mice (long *Cox7a2l* isoform) the sum of the rates of respiration on NADH- and succinate-linked substrates was equivalent to the rate in the presence of both, whereas in C57BL/6 mice (short *Cox7a2l* isoform) this was not the case. They ascribed the additive behavior in CD1 mice to the presence of separate Q pools for each pathway. However, an alternate explanation could well be that CIII+CIV catalysis is quick enough to 'keep up' with the increased rate of ubiquinone reduction.

In 2014, submitochondrial particles and membrane preparations from *Bos taurus* heart mitochondria were used to test directly whether partitioning of the Q and cyt *c* pools occur (Blaza et al., 2014). The preparations used contained a full complement of supercomplexes, with the CI and CII active sites exposed directly to added substrates. By using different amounts of cyt *c* to vary the CIII+CIV rate and thus alter the identity of the rate limiting steps for NADH and succinate oxidation, it was demonstrated how the same system, with the same

supercomplex content, could exhibit both additive and non-additive kinetics, excluding this as an argument for Q pool partitioning (Figure 5A). Furthermore, the addition of NADH, succinate, or both reductants together (in the absence of $O_2$), reduced essentially the same population of CIII, CIV and cyt *c* in every case (Figure 5B). These experiments did not reveal any additive effects and so also argue against partitioning of the Q pool. Only the spectroscopic time traces from the *b*-hemes in CIII varied significantly between the three conditions, but due to their low reduction potentials the *b*-hemes are incompletely reduced in all cases. Finally, the rate of NADH oxidation was compared with the rate of reverse electron transport, in which the proton-motive force from ATP hydrolysis is used to drive electron transport from succinate to $NAD^+$, backwards through CI (Figure 5C). The rate of reverse electron transport, which requires CI and CII to share a common Q pool, was comparable to that of NADH oxidation. Using elegant heme spectroscopy in intact living cells, others have further demonstrated that cyt *c* in *S. cerevisiae* does not face major barriers to its free diffusion (Trouillard et al., 2011), and this is consistent with all the CIV present being catalytically active, rather than only the 15-25% of it that is present in supercomplexes.

In our opinion, robust evidence for the partitioning of the Q and cyt *c* pools and for the channeling of either substrate is thus lacking. Instead, all functional and structural evidence is consistent with their free diffusion. Indeed, we contend that trapping a tiny pool of Q and cyt *c* within each supercomplex would be detrimental to respiratory chain function: it would preclude redox sensing by the pools and render the system less able to withstand individual complexes being dysfunctional. Notably, our conclusion does not support either the fluid or the solid-state model for respiratory chain organization. The original formulations of the two models linked function and structure tightly together, but this is now seen to be misleading: Q and cyt *c* diffuse between complexes or supercomplexes in any configuration. Recently, a 'plasticity model' has been proposed as a hybrid model that encompasses pool partitioning but allows the pools to overflow to give the appearance of being one (Lenaz et al., 2016), and that borrows elements from both models to be consistent with all extant data (Enríquez, 2016; Moreno-Loshuertos and Enríquez, 2016). Whereas partitioning of the Q and cyt *c* pools is a problematic concept for the reasons discussed above, the plasticity model proposes that supercomplexes are dynamic entities that are constantly dissociating and reforming, and this latter interesting aspect is worthy of further investigation.

**If not substrate channeling, what is the raison d'être of supercomplex formation?**

The existence of respiratory chain supercomplexes as structural entities is now widely accepted and it is natural to anticipate that, having evolved, they confer one or more functional advantages. Having ruled out substrate channeling, we now turn to alternative possibilities for why respiratory chain supercomplex formation is beneficial to the cell, namely: i) decreasing ROS production; ii) stabilizing or assisting in the assembly of the individual complexes; iii) regulation of respiratory chain activity; or iv) prevention of protein aggregation in the protein rich mitochondrial inner membrane.

i) CI and CIII are considered the main sites of ROS production by the respiratory chain (Murphy, 2009). Based on measurements of ROS production by isolated bovine heart mitochondria and by reconstituted liposomes containing CI and CIII either independently or in the $I/III_2$ supercomplex, and solubilized with different detergents to either maintain or disrupt the supercomplexes, Genova and coworkers proposed that supercomplex formation decreases ROS production (Maranzana et al., 2013). Being made in the presence of respiratory-chain inhibitors, their experiments refer to ROS production by the CI flavin site (Kussmaul and Hirst, 2006). However, access to the flavin site of CI is not hindered structurally by supercomplex formation, so it is difficult to rationalize the proposal. Furthermore, the ROS production rates measured were normalized using the rate of ubiquinone reduction by CI, a value that is easily modulated by changes in conditions and detergents, so lack of knowledge of the amount of CI present convolutes the interpretation. A correlation between ROS production and the level of CI present in supercomplexes has also been observed in neurons and astrocytes, cell types with very different bioenergetic properties (Lopez-Fabuel et al., 2016). For the CIII dimer, Sazanov and coworkers suggested that the asymmetry of the respirasome favors ubiquinone reduction at the $Q_i$ site closest to CIV, where locally decreased $O_2$ concentrations may decrease ROS production. However, ROS formation by CIII is dominated by the $Q_O$ site, not the $Q_i$ site (Sarewicz and Osyczka, 2015). Further work is thus required to investigate the interesting hypothesis that supercomplexes decrease ROS production.

ii) Mutations that cause defects in CIII or CIV may cause combined deficiencies in which CI is also affected (Acín-Pérez et al., 2004; Diaz et al., 2006). Because supercomplex formation/stability is often affected by the original defect, and defects in CI do not impact similarly on CIII and CIV, it has been proposed that CIII and CIV are required to stabilize CI through supercomplex formation (Acín-Pérez et al., 2004; Diaz et al., 2006; Schägger et al., 2004). First, we note the effect is not universal: there are well-known examples of fully-assembled CI being present when CIV is disrupted (Balsa et al., 2012). There are also many

human genetic conditions in which impaired CIV biogenesis leads to an isolated CIV deficiency (Diaz, 2010; Williams et al., 2004; Zhu et al., 1998), perhaps because in patients with low levels of CIV, the residual CIV is preferentially incorporated into respirasomes (Lazarou et al., 2009), and may be sufficient for their formation. Second, the effect can also be explained by a supercomplex-independent mechanism (Diaz et al., 2012; Guarás et al., 2016): when respiration is compromised (at CIII or CIV) reducing equivalents back-up into the $NAD^+$/NADH pool and ROS production by CI increases (Kussmaul and Hirst, 2006); increased ROS is detrimental to CI stability, and loss of CI (and CIII or CIV) leads to lower supercomplex levels (Diaz et al., 2012). Evidence has since been presented that the increased ROS production arises from reverse electron transfer through CI (Guarás et al., 2016), with the same consequences. Thus, these combined respiratory-chain deficiencies present no unequivocal evidence for the interdependence of the complexes through supercomplex formation.

Supercomplex formation in human cell lines has also been proposed to provide a scaffold for the completion of CI assembly (Moreno-Lastres et al., 2012). According to this model, the final section of the peripheral arm of CI (the pre-assembled NADH-oxidizing module) is only added once the nascent complex has been assembled into a supercomplex so that CI is not activated until the supercomplex is complete; this is consistent with CIII stabilizing partially-assembled CI in *Ndufs4* knockout mice (Calvaruso et al., 2012). In contrast, recent proteomics studies that combined complexome profiling with BN-PAGE analyses to provide a detailed picture of CI assembly showed that the whole complex was assembled independently, before supercomplex formation and without a supercomplex scaffold (Guerrero-Castillo et al., 2016). Interestingly, NDUFA11 (a key subunit for the interaction of CI and CIII) and the pre-assembled NADH-oxidizing module are both added in the final stage of CI assembly. However, they are structurally independent in the complex, suggesting that they do not depend on one another for their incorporation. Therefore, the different results above probably reflect different balances between the independent rates at which CI assembly is completed and intercomplex associations are formed.

iii) The assembly and disassembly of supercomplexes are increasingly described as methods of regulating respiratory chain activity. For example, it was recently reported that exercise leads to increased supercomplex formation in human skeletal muscle (Greggio et al., 2016). It has also been suggested (based on the existence of more than one Q pool) that the respiratory chain may adjust its supercomplexes to promote increased flux through CI or FAD-linked dehydrogenases and assist in switching between carbohydrate and fatty-acid metabolism

(Lapuente-Brun et al., 2013). According to this model, activation of FAD-linked pathways causes over-reduction of the putative FAD-dedicated Q pool and upregulates ROS production by reverse electron transport through CI. The increased ROS production degrades CI and breaks down respirasomes to release CIII and the putative respirasome-associated Q-pool for FAD-linked respiration (Guarás et al., 2016). One weakness of this model is that it is internally inconsistent because, despite assuming the presence of separate Q pools, reverse electron transport between CI and CII requires Q to transfer between the two. Furthermore, a supercomplex-independent mechanism can achieve the same effect simply by increased ROS production leading to CI degradation.

Many varied studies will continue to observe changes to the levels of supercomplexes present in mitochondria, and correlate these to changes in metabolic conditions, the dysfunction, instability or absence of a respiratory complex, increased oxidative stress, or a change in morphology. However, it is important to recognize that correlation does not equate to causation, and to be cautious when making mechanistic assignments on the basis of indirect observations made on highly complex systems.

iv) The mitochondrial inner membrane is extremely protein-rich, with a phospholipid content of only around 30% (Fleischer et al., 1961). Therefore, supercomplexes may have been selected for because they prevent protein nucleation and aggregation (Blaza et al., 2014). The weak protein interactions that hold them together may prevent stronger deleterious interactions that would lead to loss of function, and the supernumerary subunits of the eukaryotic complexes may have evolved to promote these weak interactions. A well-known example of a similar strategy to prevent protein aggregation is in the lens of the eye, where densely packed protein molecules maintain the gel state by interacting only weakly with one another (Slingsby et al., 2013). Indeed, it is possible that supercomplexes form only in highly packed membranes due to either concentration-dependent association, or in response to a regulatory mechanism such as the expression of supercomplex assembly factors.

## CONCLUDING REMARKS AND FUTURE RESEARCH DIRECTIONS

The organization of the respiratory chain is disrupted in a large number of human mitochondrial disorders caused by mutations in both mtDNA and nDNA (Wallace, 2010), such as Barth syndrome (McKenzie et al., 2006) and Leigh syndrome (McKenzie et al., 2007), as well as in a range of age-associated human diseases, such as heart failure (Rosca et al., 2011), and by the aging process itself (Frenzel et al., 2010; Gómez et al., 2009; Kauppila et al., 2016). A deterioration of respiratory chain supercomplex formation often forms part of the

biochemical disease phenotype, but the extent to which pathology and functional decline can be attributed to it is unclear. Recent advances in understanding the structures and organization of supercomplexes (Gu et al., 2016; Letts et al., 2016; Wu et al., 2016) now open new opportunities for testing their different proposed roles, particularly those centered on spatial organization or stability rather than catalysis. For example, it should now be possible to develop supercomplexes with enhanced interactions between the complexes, as well as to generate specific mutations that have no effect other than to disrupt supercomplex formation or stability. Biochemical studies on tightly-controlled systems in which supercomplex formation is the only variable are also required to study proposed properties such as the minimization of ROS production and the dependence on different phospholipids, in the absence of convoluting factors. Recent development of methods for reliable mitochondrial metabolomics (Chen et al., 2016) may give insights into possible metabolite changes in response to supercomplex perturbations. Continuing advances in cryo-EM tomography, single-molecule labeling techniques and super-resolution light microscopy should be exploited for detailed and dynamic studies of respiratory chain organization in intact mitochondria and whole cells. Increased understanding in this area is clearly of great importance for the future, both for basic science and for understanding the roles of oxidative phosphorylation deficiencies in human disease and ageing.

## ACKNOWLEDGEMENTS

NGL receives support from the Max Planck Society, the Swedish Research Council (2015-00418) and the Knut and Alice Wallenberg foundation. JH and JNB are supported by The Medical Research Council (U105663141 to JH).

## REFERENCES

Acín-Pérez, R., Bayona-Bafaluy, M.P., Fernández-Silva, P., Moreno-Loshuertos, R., Pérez-Martos, A., Bruno, C., Moraes, C.T., and Enriquez, J.A. (2004). Respiratory complex III is required to maintain complex I in mammalian mitochondria. Mol. Cell *13*, 805–815.

Acín-Pérez, R., Carrascoso, I., Baixauli, F., Roche-Molina, M., Latorre-Pellicer, A., Fernández-Silva, P., Mittelbrunn, M., Sanchez-Madrid, F., Pérez-Martos, A., Lowell, C.A., et al. (2014). ROS-triggered phosphorylation of complex II by Fgr kinase regulates cellular adaptation to fuel use. Cell Metab. *19*, 1020–1033.

Acín-Pérez, R., Fernández-Silva, P., Peleato, M.L., Pérez-Martos, A., and Enríquez, J.A. (2008). Respiratory active mitochondrial supercomplexes. Mol. Cell *32*, 529–539.

Althoff, T., Mills, D.J., Popot, J.-L., and Kühlbrandt, W. (2011). Arrangement of electron transport chain components in bovine mitochondrial supercomplex $I_1III_2IV_1$. EMBO J. *30*,

4652–4664.

Appelhans, T., Richter, C.P., Wilkens, V., Hess, S.T., Piehler, J., and Busch, K.B. (2012). Nanoscale organization of mitochondrial microcompartments revealed by combining tracking and localization microscopy. Nano Lett. *12*, 610–616.

Balsa, E., Marco, R., Perales-Clemente, E., Szklarczyk, R., Calvo, E., Landázuri, M.O., and Enríquez, J.A. (2012). NDUFA4 is a subunit of complex IV of the mammalian electron transport chain. Cell Metab. *16*, 378–386.

Baradaran, R., Berrisford, J.M., Minhas, G.S., and Sazanov, L.A. (2013). Crystal structure of the entire respiratory complex I. Nature *494*, 443–448.

Bazán, S., Mileykovskaya, E., Mallampalli, V.K.P.S., Heacock, P., Sparagna, G.C., and Dowhan, W. (2013). Cardiolipin-dependent reconstitution of respiratory supercomplexes from purified *Saccharomyces cerevisiae* complexes III and IV. J. Biol. Chem. *288*, 401–411.

Bianchi, C., Genova, M.L., Parenti Castelli, G., and Lenaz, G. (2004). The mitochondrial respiratory chain is partially organized in a supercomplex assembly: kinetic evidence using flux control analysis. J. Biol. Chem. *279*, 36562–36569.

Blaza, J.N., Serreli, R., Jones, A.J.Y., Mohammed, K., and Hirst, J. (2014). Kinetic evidence against partitioning of the ubiquinone pool and the catalytic relevance of respiratory-chain supercomplexes. Proc. Natl. Acad. Sci. USA *111*, 15735–15740.

Böttinger, L., Horvath, S.E., Kleinschroth, T., Hunte, C., Daum, G., Pfanner, N., and Becker, T. (2012). Phosphatidylethanolamine and cardiolipin differentially affect the stability of mitochondrial respiratory chain supercomplexes. J. Mol. Biol. *423*, 677–686.

Busch, K.B., Deckers-Hebestreit, G., Hanke, G.T., and Mulkidjanian, A.Y. (2013). Dynamics of bioenergetic microcompartments. Biol. Chem. *394*, 163–188.

Calvaruso, M.A., Willems, P., van den Brand, M., Valsecchi, F., Kruse, S., Palmiter, R., Smeitink, J., and Nijtmans, L. (2011). Mitochondrial complex III stabilizes complex I in the absence of NDUFS4 to provide partial activity. Hum. Mol. Genet. *21*, 115–120.

Champagne, D.P., Hatle, K.M., Fortner, K.A., D'Alessandro, A., Thornton, T.M., Yang, R., Torralba, D., Tomás-Cortázar, J., Jun, Y.W., Ahn, K.H., et al. (2016). Fine-tuning of CD8(+) T Cell mitochondrial metabolism by the respiratory chain repressor MCJ dictates protection to influenza virus. Immunity *44*, 1299–1311.

Chen, W.W., Freinkman, E., Wang, T., Birsoy, K., and Sabatini, D.M. (2016). Absolute quantification of matrix metabolites reveals the dynamics of mitochondrial metabolism. Cell *166*, 1324–1337.

Chen, Y.-C., Taylor, E.B., Dephoure, N., Heo, J.-M., Tonhato, A., Papandreou, I., Nath, N., Denko, N.C., Gygi, S.P., and Rutter, J. (2012). Identification of a protein mediating respiratory supercomplex stability. Cell Metab. *15*, 348–360.

Cogliati, S., Calvo, E., Loureiro, M., Guaras, A.M., Nieto-Arellano, R., Garcia-Poyatos, C., Ezkurdia, I., Mercader, N., Vazquez, J., and Enríquez, J.A. (2016). Mechanism of super-assembly of respiratory complexes III and IV. Nature *539, 579-582*.

Cogliati, S., Frezza, C., Soriano, M.E., Varanita, T., Quintana-Cabrera, R., Corrado, M., Cipolat, S., Costa, V., Casarin, A., Gomes, L.C., et al. (2013). Mitochondrial cristae shape determines respiratory chain supercomplexes assembly and respiratory efficiency. Cell *155*, 160–171.

Davies, K.M., Strauss, M., Daum, B., Kief, J.H., Osiewacz, H.D., Rycovska, A., Zickermann, V., and Kühlbrandt, W. (2011). Macromolecular organization of ATP synthase and complex I in whole mitochondria. Proc. Natl. Acad. Sci. USA *108*, 14121–14126.

Desmurs, M., Foti, M., Raemy, E., Vaz, F.M., Martinou, J.-C., Bairoch, A., and Lane, L. (2015). C11orf83, a mitochondrial cardiolipin-binding protein involved in $bc_1$ complex assembly and supercomplex stabilization. Mol. Cell. Biol. *35*, 1139–1156.

Diaz, F. (2010). Cytochrome *c* oxidase deficiency: patients and animal models. Biochim. Biophys. Acta *1802*, 100–110.

Diaz, F., Enríquez, J.A., and Moraes, C.T. (2012). Cells lacking Rieske iron-sulfur protein have a reactive oxygen species-associated decrease in respiratory complexes I and IV. Mol. Cell. Biol. *32*, 415–429.

Diaz, F., Fukui, H., Garcia, S., and Moraes, C.T. (2006). Cytochrome *c* oxidase is required for the assembly/stability of respiratory complex I in mouse fibroblasts. Mol. Cell. Biol. *26*, 4872–4881.

Dudkina, N.V., Eubel, H., Keegstra, W., Boekema, E.J., and Braun, H.-P. (2005). Structure of a mitochondrial supercomplex formed by respiratory-chain complexes I and III. Proc. Natl. Acad. Sci. USA *102*, 3225–3229.

Dudkina, N.V., Kouril, R., Peters, K., Braun, H.-P., and Boekema, E.J. (2010). Structure and function of mitochondrial supercomplexes. Biochim. Biophys. Acta *1797*, 664–670.

Dudkina, N.V., Kudryashev, M., Stahlberg, H., and Boekema, E.J. (2011). Interaction of complexes I, III, and IV within the bovine respirasome by single particle cryoelectron tomography. Proc. Natl. Acad. Sci. USA *108*, 15196–15200.

Enríquez, J.A. (2016). Supramolecular organization of respiratory complexes. Annu. Rev. Physiol. *78*, 533–561.

Ernster, L., and Schatz, G. (1981). Mitochondria: a historical review. J. Cell Biol. *91*, 227s–255s.

Eubel, H., Jänsch, L., and Braun, H.-P. (2003). New insights into the respiratory chain of plant mitochondria. Supercomplexes and a unique composition of complex II. Plant Physiol. *133*, 274–286.

Fell, D.A. (1992). Metabolic control analysis: a survey of its theoretical and experimental development. Biochem. J. *286*, 313–330.

Fernandez-Leiro, R., and Scheres, S.H.W. (2016). Unravelling biological macromolecules with cryo-electron microscopy. Nature *537*, 339–346.

Fiedorczuk, K., Letts, J.A., Degliesposti, G., Kaszuba, K., Skehel, M., and Sazanov, L.A.

(2016). Atomic structure of the entire mammalian mitochondrial complex I. Nature *538*, 406–410.

Fleischer, S., Klouwen, H., and Brierley, G. (1961). Studies of the electron transfer system. 38. Lipid composition of purified enzyme preparations derived from beef heart mitochondria. J. Biol. Chem. *236*, 2936–2941.

Frenzel, M., Rommelspacher, H., Sugawa, M.D., and Dencher, N.A. (2010). Ageing alters the supramolecular architecture of OxPhos complexes in rat brain cortex. Exp. Gerontol. *45*, 563–572.

Gilkerson, R.W., Selker, J.M.L., and Capaldi, R.A. (2003). The cristal membrane of mitochondria is the principal site of oxidative phosphorylation. FEBS Lett. *546*, 355–358.

Gómez, L.A., Monette, J.S., Chavez, J.D., Maier, C.S., and Hagen, T.M. (2009). Supercomplexes of the mitochondrial electron transport chain decline in the aging rat heart. Arch. Biochem. Biophys. *490*, 30–35.

Greggio, C., Jha, P., Kulkarni, S.S., Lagarrigue, S., Broskey, N.T., Boutant, M., Wang, X., Conde Alonso, S., Ofori, E., Auwerx, J., et al. (2016). Enhanced respiratory chain supercomplex formation in response to exercise in human skeletal muscle. Cell Metab. *25*, 1-11.

Gu, J., Wu, M., Guo, R., Yan, K., Lei, J., Gao, N., and Yang, M. (2016). The architecture of the mammalian respirasome. Nature *537*, 639–643.

Guarás, A., Perales-Clemente, E., Calvo, E., Acín-Pérez, R., Loureiro-Lopez, M., Pujol, C., Martínez-Carrascoso, I., Nuñez, E., García-Marqués, F., Rodríguez-Hernández, M.A., et al. (2016). The $CoQH_2$/CoQ ratio serves as a sensor of respiratory chain efficiency. Cell Rep. *15*, 197–209.

Guerrero-Castillo, S., Baertling, F., Kownatzki, D., Wessels, H.J., Arnold, S., Brandt, U., and Nijtmans, L. (2016). The assembly pathway of mitochondrial respiratory chain complex I. Cell Metab. *25*, 1-12.

Gupte, S.S., and Hackenbrock, C.R. (1988). The role of cytochrome *c* diffusion in mitochondrial electron transport. J. Biol. Chem. *263*, 5248–5253.

Hackenbrock, C.R., Chazotte, B., and Gupte, S.S. (1986). The random collision model and a critical assessment of diffusion and collision in mitochondrial electron transport. J. Bioenerg. Biomembr. *18*, 331–368.

Hatle, K.M., Gummadidala, P., Navasa, N., Bernardo, E., Dodge, J., Silverstrim, B., Fortner, K., Burg, E., Suratt, B.T., Hammer, J., et al. (2013). MCJ/DnaJC15, an endogenous mitochondrial repressor of the respiratory chain that controls metabolic alterations. Mol. Cell. Biol. *33*, 2302–2314.

Hayashi, T., Asano, Y., Shintani, Y., Aoyama, H., Kioka, H., Tsukamoto, O., Hikita, M., Shinzawa-Itoh, K., Takafuji, K., Higo, S., et al. (2015). *Higd1a* is a positive regulator of cytochrome *c* oxidase. Proc. Natl. Acad. Sci. USA *112*, 1553–1558.

Heinemeyer, J., Braun, H.-P., Boekema, E.J., and Kouril, R. (2007). A structural model of the

cytochrome *c* reductase/oxidase supercomplex from yeast mitochondria. J. Biol. Chem. *282*, 12240–12248.

Ikeda, K., Shiba, S., Horie-Inoue, K., Shimokata, K., and Inoue, S. (2013). A stabilizing factor for mitochondrial respiratory supercomplex assembly regulates energy metabolism in muscle. Nat. Commun. *4*, 2147.

Iwata, S., Lee, J.W., Okada, K., Lee, J.K., Iwata, M., Rasmussen, B., Link, T.A., Ramaswamy, S., and Jap, B.K. (1998). Complete structure of the 11-subunit bovine mitochondrial cytochrome $bc_1$ complex. Science *281*, 64–71.

Jha, P., Wang, X., and Auwerx, J. (2016). Analysis of mitochondrial respiratory chain supercomplexes using blue native polyacrylamide gel electrophoresis (BN-PAGE). Curr. Protoc. Mouse Biol. *6*, 1–14.

Kauppila, T.E.S., Kauppila, J.H.K., and Larsson, N.-G. (2016). Mammalian mitochondria and aging: an update. Cell Metab. *25,* 1–15.

Keilin, D., and Hartree, E.F. (1947). Activity of the cytochrome system in heart muscle preparations. Biochem. J. *41*, 500–502.

Kröger, A., and Klingenberg, M. (1966). On the role of ubiquinone in mitochondria. II. Redox reactions of ubiquinone under the control of oxidative phosphorylation. Biochem. Z. *344*, 317–336.

Kröger, A., and Klingenberg, M. (1973). Further evidence for the pool function of ubiquinone as derived from the inhibition of the electron transport by antimycin. Eur. J. Biochem. *39*, 313–323.

Kussmaul, L., and Hirst, J. (2006). The mechanism of superoxide production by NADH:ubiquinone oxidoreductase (complex I) from bovine heart mitochondria. Proc. Natl. Acad. Sci. USA *103*, 7607–7612.

Lange, C., and Hunte, C. (2002). Crystal structure of the yeast cytochrome $bc_1$ complex with its bound substrate cytochrome *c*. Proc. Natl. Acad. Sci. USA *99*, 2800–2805.

Lapuente-Brun, E., Moreno-Loshuertos, R., Acín-Pérez, R., Latorre-Pellicer, A., Colás, C., Balsa, E., Perales-Clemente, E., Quirós, P.M., Calvo, E., Rodríguez-Hernández, M.A., et al. (2013). Supercomplex assembly determines electron flux in the mitochondrial electron transport chain. Science *340*, 1567–1570.

Lazarou, M., Smith, S.M., Thorburn, D.R., Ryan, M.T., and McKenzie, M. (2009). Assembly of nuclear DNA-encoded subunits into mitochondrial complex IV and their preferential integration into supercomplex forms in patient mitochondria. FEBS J. *276*, 6701–6713.

Lenaz, G., Tioli, G., Falasca, A.I., and Genova, M.L. (2016). Complex I function in mitochondrial supercomplexes. Biochim. Biophys. Acta *1857*, 991–1000.

Letts, J.A., Fiedorczuk, K., and Sazanov, L.A. (2016). The architecture of respiratory supercomplexes. Nature *537*, 644–648.

Llorente-Garcia, I., Lenn, T., Erhardt, H., Harriman, O.L., Liu, L.-N., Robson, A., Chiu, S.-W.,

Matthews, S., Willis, N.J., Bray, C.D., et al. (2014). Single-molecule *in vivo* imaging of bacterial respiratory complexes indicates delocalized oxidative phosphorylation. Biochim. Biophys. Acta *1837*, 811–824.

Lopez-Fabuel, I., Le Douce, J., Logan, A., James, A.M., Bonvento, G., Murphy, M.P., Almeida, A., and Bolaños, J.P. (2016). Complex I assembly into supercomplexes determines differential mitochondrial ROS production in neurons and astrocytes. Proc. Natl. Acad. Sci. USA *113*, 13063–13068.

Maranzana, E., Barbero, G., Falasca, A.I., Lenaz, G., and Genova, M.L. (2013). Mitochondrial respiratory supercomplex association limits production of reactive oxygen species from complex I. Antioxid. Redox Signal. *19*, 1469–1480.

McKenzie, M., Lazarou, M., Thorburn, D.R., and Ryan, M.T. (2006). Mitochondrial respiratory chain supercomplexes are destabilized in Barth Syndrome patients. J. Mol. Biol. *361*, 462–469.

McKenzie, M., Lazarou, M., Thorburn, D.R., and Ryan, M.T. (2007). Analysis of mitochondrial subunit assembly into respiratory chain complexes using Blue Native polyacrylamide gel electrophoresis. Anal. Biochem. *364*, 128–137.

Milenkovic, D., and Larsson, N.-G. (2015). Mic10 oligomerization pinches off mitochondrial cristae. Cell Metab. *21*, 660–661.

Milenkovic, D., Matic, S., Kühl, I., Ruzzenente, B., Freyer, C., Jemt, E., Park, C.B., Falkenberg, M., and Larsson, N.-G. (2013). TWINKLE is an essential mitochondrial helicase required for synthesis of nascent D-loop strands and complete mtDNA replication. Hum. Mol. Genet. *22*, 1983-1993.

Mileykovskaya, E., and Dowhan, W. (2009). Cardiolipin membrane domains in prokaryotes and eukaryotes. Biochim. Biophys. Acta *1788*, 2084–2091.

Mileykovskaya, E., and Dowhan, W. (2013). Cardiolipin-dependent formation of mitochondrial respiratory supercomplexes. Chem. Phys. Lipids. *179*, 42-48.

Mileykovskaya, E., Penczek, P.A., Fang, J., Mallampalli, V.K.P.S., Sparagna, G.C., and Dowhan, W. (2012). Arrangement of the respiratory chain complexes in *Saccharomyces cerevisiae* supercomplex $III_2IV_2$ revealed by single particle cryo-electron microscopy. J. Biol. Chem. *287*, 23095–23103.

Mitchell, P. (1961). Coupling of phosphorylation to electron and hydrogen transfer by a chemi-osmotic type of mechanism. Nature *191*, 144–148.

Mitchell, P. (1975). The protonmotive Q cycle: a general formulation. FEBS Lett. *59*, 137–139.

Mitsopoulos, P., Chang, Y.-H., Wai, T., König, T., Dunn, S.D., Langer, T., and Madrenas, J. (2015). Stomatin-like protein-2 is required for *in vivo* mitochondrial respiratory chain supercomplex formation and optimal cell function. Mol. Cell. Biol. *35*, 1838-1847.

Moreno-Lastres, D., Fontanesi, F., García-Consuegra, I., Martín, M.A., Arenas, J., Barrientos, A., and Ugalde, C. (2012). Mitochondrial complex I plays an essential role in human

respirasome assembly. Cell Metab. *15*, 324–335.

Moreno-Loshuertos, R., and Enríquez, J.A. (2016). Respiratory supercomplexes and the functional segmentation of the CoQ pool. Free Radic. Biol. Med. *100*, 5-13.

Mourier, A., Matic, S., Ruzzenente, B., Larsson, N.-G., and Milenkovic, D. (2014). The respiratory chain supercomplex organization is independent of COX7a2l isoforms. Cell Metab. *20*, 1069–1075.

Murphy, M.P. (2009). How mitochondria produce reactive oxygen species. Biochem. J. *417*, 1–13.

Nicholls, D.G., and Ferguson, S. (2013). Bioenergetics 4th edition (Elsevier Ltd).

Pérez-Pérez, R., Lobo-Jarne, T., Milenkovic, D., Mourier, A., Bratic, A., García-Bartolomé, A., Fernández-Vizarra, E., Cadenas, S., Delmiro, A., García-Consuegra, I., et al. (2016). COX7A2L is a mitochondrial complex III binding protein that stabilizes the III2+IV supercomplex without affecting respirasome formation. Cell Rep. *16*, 2387–2398.

Pfanner, N., van der Laan, M., Amati, P., Capaldi, R.A., Caudy, A.A., Chacinska, A., Darshi, M., Deckers, M., Hoppins, S., Icho, T., et al. (2014). Uniform nomenclature for the mitochondrial contact site and cristae organizing system. J. Cell Biol. *204*, 1083–1086.

Pfeiffer, K., Gohil, V., Stuart, R.A., Hunte, C., Brandt, U., Greenberg, M.L., and Schägger, H. (2003). Cardiolipin stabilizes respiratory chain supercomplexes. J. Biol. Chem. *278*, 52873–52880.

Picard, M., Wallace, D.C., and Burelle, Y. (2016). The rise of mitochondria in medicine. Mitochondrion *30*, 105–116.

Rich, P.R. (1984). Electron and proton transfers through quinones and cytochrome *bc* complexes. Biochim. Biophys. Acta *768*, 53–79.

Rosca, M., Minkler, P., and Hoppel, C.L. (2011). Cardiac mitochondria in heart failure: normal cardiolipin profile and increased threonine phosphorylation of complex IV. Biochim. Biophys. Acta *1807*, 1373–1382.

Rydström Lundin, C., Ballmoos, von, C., Ott, M., Ädelroth, P., and Brzezinski, P. (2016). Regulatory role of the respiratory supercomplex factors in *Saccharomyces cerevisiae*. Proc. Natl. Acad. Sci. USA *113*, E4476–E4485.

Sarewicz, M., and Osyczka, A. (2015). Electronic connection between the quinone and cytochrome *c* redox pools and its role in regulation of mitochondrial electron transport and redox signaling. Physiol. Rev. *95*, 219–243.

Schägger, H., and Pfeiffer, K. (2000). Supercomplexes in the respiratory chains of yeast and mammalian mitochondria. EMBO J. *19*, 1777–1783.

Schägger, H., and Pfeiffer, K. (2001). The ratio of oxidative phosphorylation complexes I-V in bovine heart mitochondria and the composition of respiratory chain supercomplexes. J. Biol. Chem. *276*, 37861–37867.

Schägger, H., de Coo, R., Bauer, M.F., Hofmann, S., Godinot, C., and Brandt, U. (2004).

Significance of respirasomes for the assembly/stability of human respiratory chain complex I. J. Biol. Chem. *279*, 36349–36353.

Scheres, S.H.W. (2016). Processing of structurally heterogeneous cryo-EM data in RELION. Meth. Enzymol. *579*, 125–157.

Schlame, M., and Greenberg, M.L. (2017). Biosynthesis, remodeling and turnover of mitochondrial cardiolipin. Biochim. Biophys. Acta *1862*, 3–7.

Schneider, H., Lemasters, J.J., and Hackenbrock, C.R. (1982). Lateral diffusion of ubiquinone during electron transfer in phospholipid- and ubiquinone-enriched mitochondrial membranes. J. Biol. Chem. *257*, 10789–10793.

Schneider, H., Lemasters, J.J., Höchli, M., and Hackenbrock, C.R. (1980). Liposome-mitochondrial inner membrane fusion. Lateral diffusion of integral electron transfer components. J. Biol. Chem. *255*, 3748–3756.

Shimada, S., Shinzawa-Itoh, K., Baba, J., Aoe, S., Shimada, A., Yamashita, E., Kang, J., Tateno, M., Yoshikawa, S., and Tsukihara, T. (2016). Complex structure of cytochrome *c*-cytochrome *c* oxidase reveals a novel protein-protein interaction mode. EMBO J. e201695021. doi:10.15252/embj.201695021.

Sinha, D., Srivastava, S., and D'Silva, P. (2016). Functional diversity of human mitochondrial J-proteins is independent of their association with the inner membrane presequence translocase. J. Biol. Chem. *291*, 17345–17359.

Slingsby, C., Wistow, G.J., and Clark, A.R. (2013). Evolution of crystallins for a role in the vertebrate eye lens. Protein Sci. *22*, 367–380.

Sousa, J.S., Mills, D.J., Vonck, J., and Kühlbrandt, W. (2016). Functional asymmetry and electron flow in the bovine respirasome. eLife *5*, e21290.

Sterky, F.H., Hoffman, A.F., Milenkovic, D., Bao, B., Paganelli, A., Edgar, D., Wibom, R., Lupica, C.R., Olson, L., and Larsson, N.-G. (2012). Altered dopamine metabolism and increased vulnerability to MPTP in mice with partial deficiency of mitochondrial complex I in dopamine neurons. Hum. Mol. Genet. *21*, 1078–1089.

Strauss, M., Hofhaus, G., Schröder, R.R., and Kühlbrandt, W. (2008). Dimer ribbons of ATP synthase shape the inner mitochondrial membrane. EMBO J. *27*, 1154–1160.

Strogolova, V., Furness, A., Robb-McGrath, M., Garlich, J., and Stuart, R.A. (2012). Rcf1 and Rcf2, members of the hypoxia-induced gene 1 protein family, are critical components of the mitochondrial cytochrome $bc_1$-cytochrome *c* oxidase supercomplex. Mol. Cell. Biol. *32*, 1363–1373.

Stroh, A., Anderka, O., Pfeiffer, K., Yagi, T., Finel, M., Ludwig, B., and Schägger, H. (2004). Assembly of respiratory complexes I, III, and IV into NADH oxidase supercomplex stabilizes complex I in *Paracoccus denitrificans*. J. Biol. Chem. *279*, 5000–5007.

Stroud, D.A., Surgenor, E.E., Formosa, L.E., Reljic, B., Frazier, A.E., Dibley, M.G., Osellame, L.D., Stait, T., Beilharz, T.H., Thorburn, D.R., et al. (2016). Accessory subunits are integral for assembly and function of human mitochondrial complex I. Nature *538*, 123–126.

Trouillard, M., Meunier, B., and Rappaport, F. (2011). Questioning the functional relevance of mitochondrial supercomplexes by time-resolved analysis of the respiratory chain. Proc. Natl. Acad. Sci. USA *108*, E1027–E1034.

Tsukihara, T., Aoyama, H., Yamashita, E., Tomizaki, T., Yamaguchi, H., Shinzawa-Itoh, K., Nakashima, R., Yaono, R., and Yoshikawa, S. (1996). The whole structure of the 13-subunit oxidized cytochrome *c* oxidase at 2.8 Å. Science *272*, 1136–1144.

Vinothkumar, K.R., Zhu, J., and Hirst, J. (2014). Architecture of mammalian respiratory complex I. Nature *515*, 80–84.

Vogel, F., Bornhovd, C., Neupert, W., and Reichert, A.S. (2006). Dynamic subcompartmentalization of the mitochondrial inner membrane. J. Cell Biol. *175*, 237–247.

Vukotic, M., Oeljeklaus, S., Wiese, S., Vögtle, F.-N., Meisinger, C., Meyer, H.E., Zieseniss, A., Katschinski, D.M., Jans, D.C., Jakobs, S., et al. (2012). Rcf1 mediates cytochrome oxidase assembly and respirasome formation, revealing heterogeneity of the enzyme complex. Cell Metab. *15*, 336–347.

Wallace, D.C. (2010). Mitochondrial DNA mutations in disease and aging. Environ. Mol. Mutagen. *51*, 440-450.

Wan, W., and Briggs, J.A.G. (2016). Cryo-electron tomography and subtomogram averaging. Meth. Enzymol. *579*, 329–367.

Warburg, O. (1928). The chemical constitution of respiration ferment. Science *68*, 437–443.

Weeks, A., Lund, L., and Raushel, F.M. (2006). Tunneling of intermediates in enzyme-catalyzed reactions. Curr. Opin. Chem. Biol. *10*, 465–472.

Wilkens, V., Kohl, W., and Busch, K. (2013). Restricted diffusion of OXPHOS complexes in dynamic mitochondria delays their exchange between cristae and engenders a transitory mosaic distribution. J. Cell. Sci. *126*, 103–116.

Williams, E.G., Wu, Y., Jha, P., Dubuis, S., Blattmann, P., Argmann, C.A., Houten, S.M., Amariuta, T., Wolski, W., Zamboni, N., et al. (2016). Systems proteomics of liver mitochondria function. Science *352*, aad0189.

Williams, S.L., Valnot, I., Rustin, P., and Taanman, J.-W. (2004). Cytochrome *c* oxidase subassemblies in fibroblast cultures from patients carrying mutations in COX10, SCO1, or SURF1. J. Biol. Chem. *279*, 7462–7469.

Wu, M., Gu, J., Guo, R., Huang, Y., and Yang, M. (2016). Structure of mammalian respiratory supercomplex $I_1III_2IV_1$. Cell *167*, 1598–1609.

Xu, Y., Phoon, C.K.L., Berno, B., D'Souza, K., Hoedt, E., Zhang, G., Neubert, T.A., Epand, R.M., Ren, M., and Schlame, M. (2016). Loss of protein association causes cardiolipin degradation in Barth syndrome. Nat. Chem. Biol. *12*, 641–647.

Zhang, M., Mileykovskaya, E., and Dowhan, W. (2005). Cardiolipin is essential for organization of complexes III and IV into a supercomplex in intact yeast mitochondria. J. Biol. Chem. *280*, 29403–29408.

Zhu, J., Vinothkumar, K.R., and Hirst, J. (2016). Structure of mammalian respiratory complex I. Nature *536*, 354–358.

Zhu, Z., Yao, J., Johns, T., Fu, K., De Bie, I., Macmillan, C., Cuthbert, A.P., Newbold, R.F., Wang, J., Chevrette, M., et al. (1998). SURF1, encoding a factor involved in the biogenesis of cytochrome *c* oxidase, is mutated in Leigh syndrome. Nat. Genet. *20*, 337–343.

## FIGURE AND TABLE LEGENDS

**Figure 1. Structures of the respirasome.** A) The arrangement of CI (orange), the CIII dimer (the monomers are shown in blue and cyan), and CIV (magenta) in the porcine respirasome, viewed along the membrane plane. B) The porcine respirasome viewed from the matrix. C) Comparison of the porcine and ovine respirasome structures. The structures were superimposed using the structure of the CIII dimer, to reveal the different relative positions of CI and CIV. CIV is shown as transparent over-lapping shapes (pink, porcine respirasome; magenta, tight ovine respirasome; blue, loose ovine respirasome). The transmembrane helix in CIV COX7A is highlighted to show how it moves relative to CIII UQCR11, which has been modeled in two slightly different positions. The figure was created using 5GPN.pdb (Gu et al., 2016) (provided by the authors before release by the protein data bank), 5J4Z.pdb and 5J7Y.pdb (Letts et al., 2016).

**Figure 2. The presence of supercomplexes and respirasomes depends on COX7A2L and cardiolipin.** A) The respiratory chain complexes of mouse strains harboring the long COX7A2L isoform (e.g. CD1 and BALB/c) are organized in respirasomes ($I/III_2/IV$) and supercomplexes ($I/III_2$ and $III_2/IV$). B) Strains carrying the short COX7A2L isoform (e.g. C57BL/6 and DBA/2J) lack the $III_2/IV$ supercomplex. C) Deficiency of the mitochondrial signature phospholipid, cardiolipin, leads to destabilized supercomplex assemblies (light colors).

**Figure 3. Proposal for how respirasomes form in the presence and absence of the long isoform of COX7A2L.** A) Respirasome formation in the presence of the long isoform of COX7A2L. Top: the individual, fully-assembled complexes are CI, the CIII dimer and the CIV monomer. COX7A2L is weakly associated with CIII (it is not observed in the structure of CIII) and is proposed to interact with subunit UQCR11. COX7A is also shown as a CIV subunit.

Middle: a tight interface forms between CIII and CIV when COX7A2L replaces COX7A. Bottom: the $III_2$/IV supercomplex associates with CI to form the respirasome. It is also possible that CIII and CIV both associate with CI before the $III_2$/IV interface forms. B) Respirasome formation in the absence of the long isoform of COX7A2L. i) The individual, fully-assembled complexes are CI, the CIII dimer and the CIV monomer. COX7A is shown as a CIV subunit. ii) CIII and CIV both associate with CI but a tight interface is not formed between them. The $III_2$/IV supercomplex is unstable.

**Figure 4. Ubiquinone and cyt *c* binding sites in the respirasome.** A) The transmembrane helices in the respirasome, shown in the same orientation as Figure 1B. The exit from the CI ubiquinone-binding site is indicated, along with the positions of the two ubiquinol-binding sites in CIII. B) The respirasome viewed from the intermembrane space with two cyt *c* molecules shown to approximately indicate their binding sites on CIII, and the negatively-charged patch on CIV where the reduced cyt *c* is reoxidized. The figure was created using 5GPN.pdb for the porcine respirasome (Gu et al., 2016) (provided by the authors before release by the protein data bank).

**Figure 5. Functional data that demonstrate there is only one Q pool in the inner mitochondrial membrane.** A). Rates of $O_2$ reduction by submitochondrial particles (SMPs) measured using NADH, succinate, or both substrates together. The sum of the individually-measured rates is also shown. For SMPs prepared with additional cyt *c*, the rate of CIII+CIV catalysis is high so adding both substrates together increases the overall rate. For SMPs prepared without additional cyt c, the rate of CIII+CIV catalysis is low so the rate of $O_2$ reduction is constant, regardless of which substrate(s) are added. B). Reduction of the cyt $c_1$ heme in CIII and of cyt *c* upon addition of NADH, succinate, or both substrates together, followed spectroscopically. The relative extents of reduction are indicated for the ends of the traces shown and in all cases the hemes are close to fully reduced. C). The rates of different reactions measured in the same set of SMPs. Electrons can pass from CII to CI (in reverse electron transport) as fast as from CI to CIII+IV. Reverse electron transport from succinate to $NAD^+$ requires ATP hydrolysis to overcome the potential difference. Data from Hirst and coworkers (Blaza et al., 2014).

**Table 1. Overview of the literature on the supercomplex organization in C57BL/6 mouse strain harboring the short *Cox7a2l* isoform.** +, present; -, absent; n.d., not determined.

| Study | Mouse tissue (C57BL/6 background) | Supercomplex $III_2/IV_1$ | Respirasomes $I/III_n/IV_n$ |
|---|---|---|---|
| Lapuenete-Brun et al., 2013 | liver | - | - |
| Ikeda et al., 2013 | sk. muscle | n.d. | + |
| Mourier et al., 2014 | heart / liver | - | + |
| Jha et al, 2016 | Liver | - | + |
| Williams et al., 2016 | liver / heart | - | + |
| Perez-Perez et al., 2016 | heart | - | + |
| Cogliati et al., 2016 | heart / sk. muscle | - | + |
| | liver / kidney / brain | - | - |

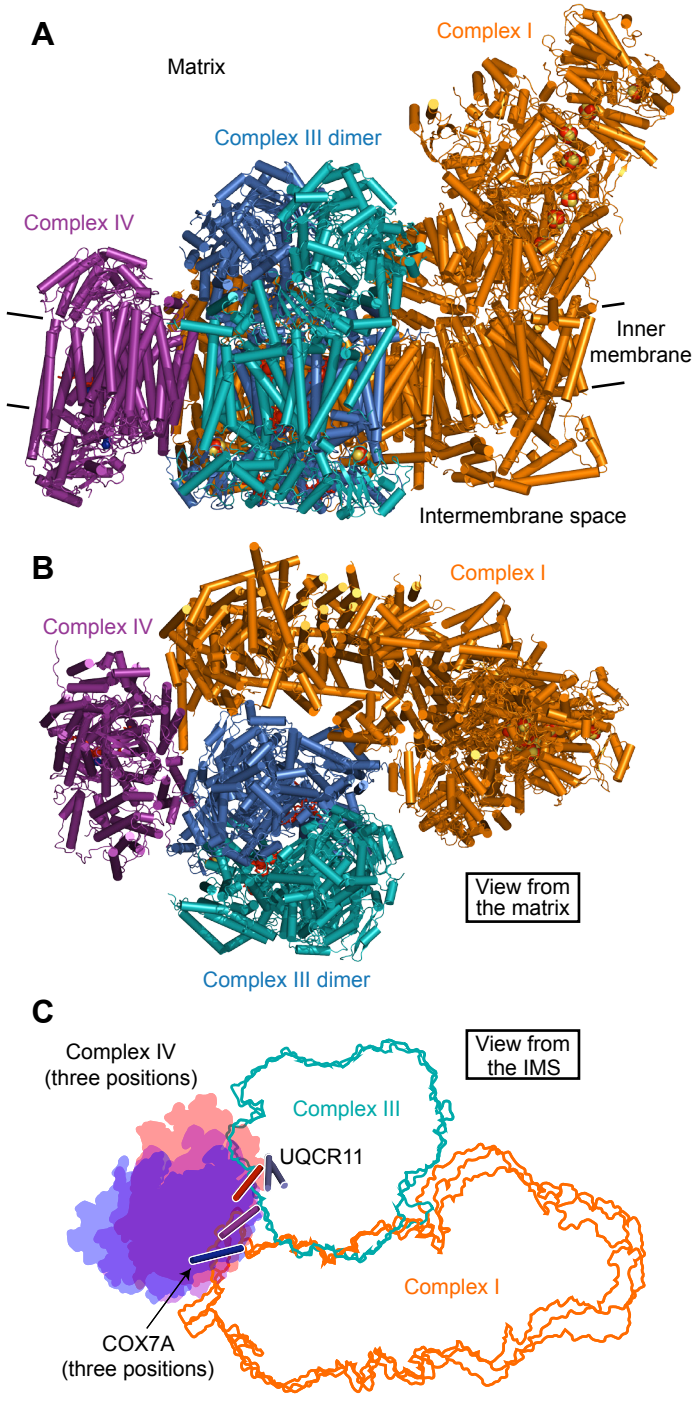
A
Matrix
Complex I
Complex III dimer
Complex IV
Inner membrane
Intermembrane space
B
Complex I
Complex IV
View from the matrix
Complex III dimer
C
Complex IV (three positions)
View from the IMS
Complex III
UQCR11
Complex I
COX7A (three positions)

Figure 1

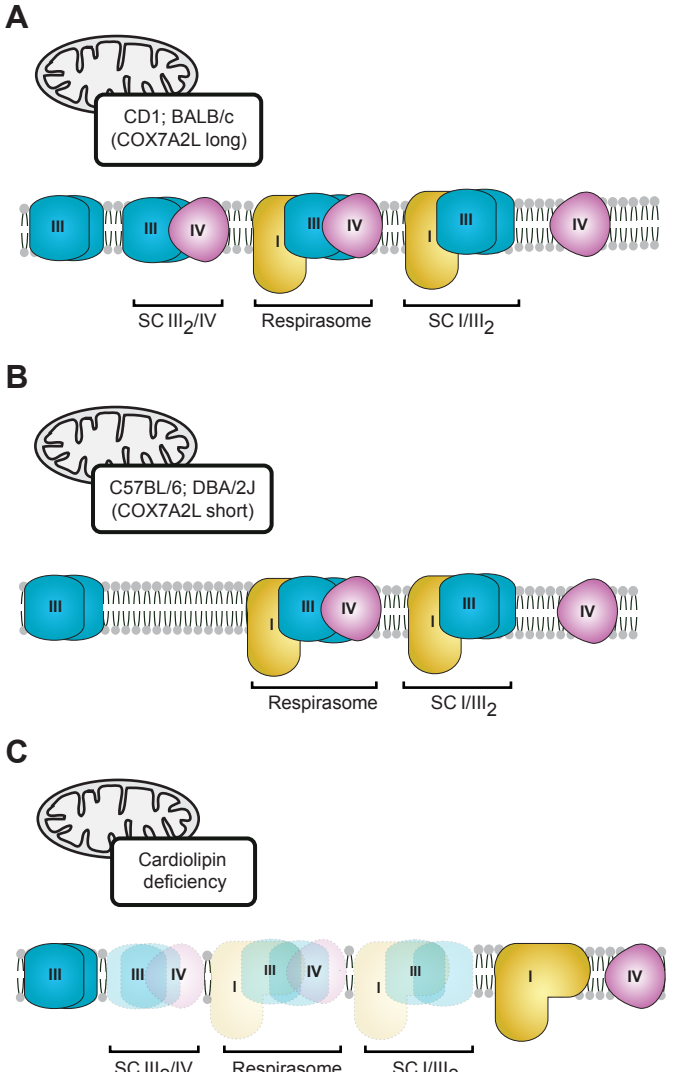
A
CD1; BALB/c
(COX7A2L long)
III
III
IV
I
III
IV
I
III
IV
SC III2/IV
Respirasome
SC I/III2
B
C57BL/6; DBA/2J
(COX7A2L short)
III
I
III
IV
I
III
IV
Respirasome
SC I/III2
C
Cardiolipin
deficiency
III
III
IV
I
III
IV
I
III
I
IV
SC III2/IV
Respirasome
SC I/III2

Figure 2

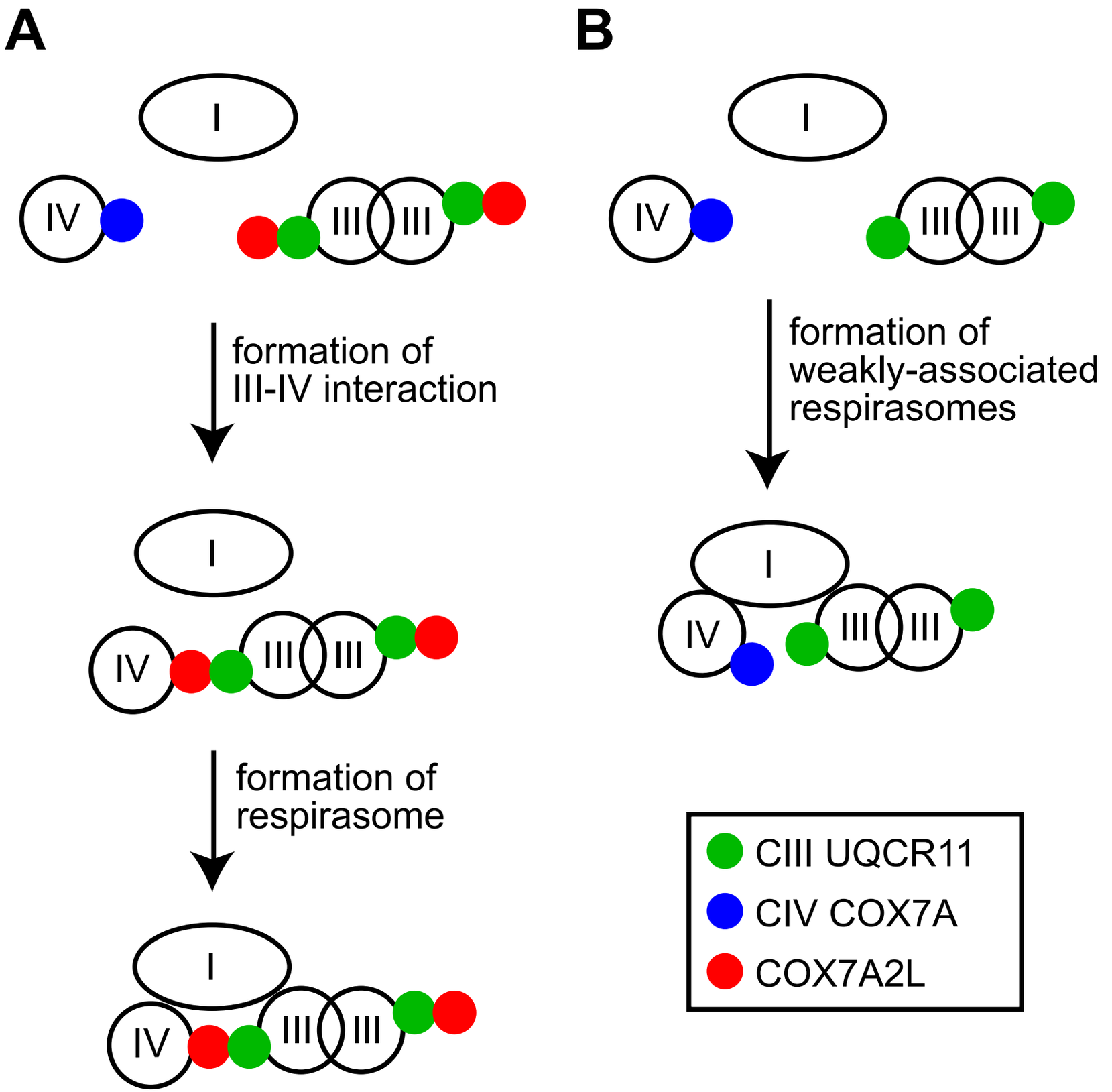
A
I
IV
III
III
formation of
III-IV interaction
I
IV
III
III
formation of
respirasome
I
IV
III
III
B
I
IV
III
III
formation of
weakly-associated
respirasomes
I
IV
III
III
CIII UQCR11
CIV COX7A
COX7A2L

Figure 3

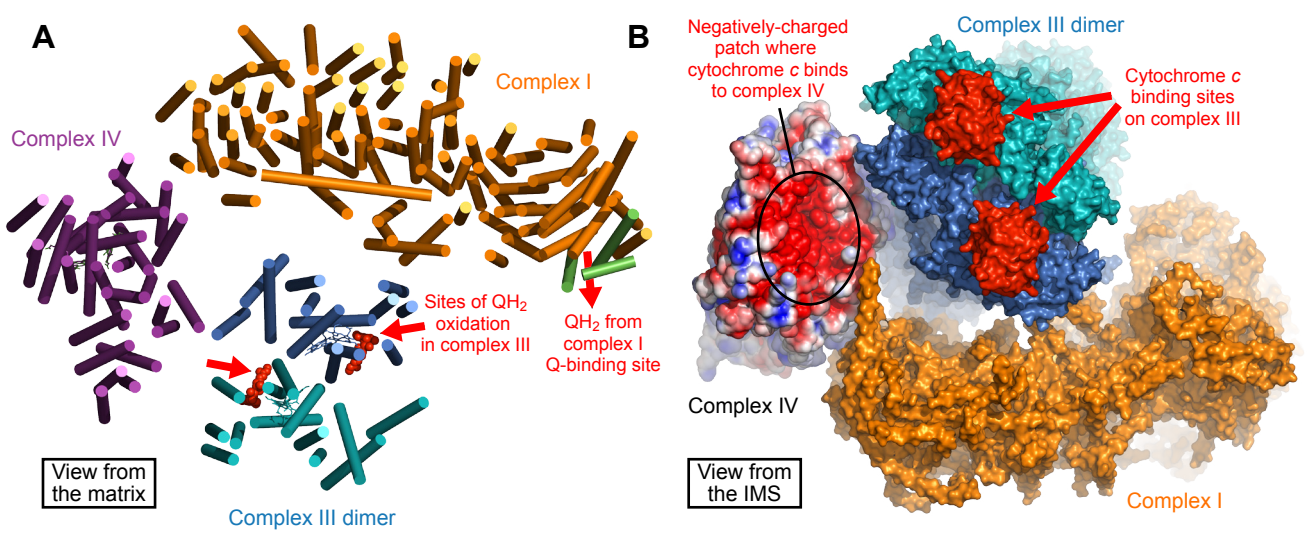
A
Complex I
Complex IV
Sites of $QH_2$ oxidation in complex III
$QH_2$ from complex I Q-binding site
View from the matrix
Complex III dimer
B
Negatively-charged patch where cytochrome *c* binds to complex IV
Complex III dimer
Cytochrome *c* binding sites on complex III
Complex IV
View from the IMS
Complex I

Figure 4

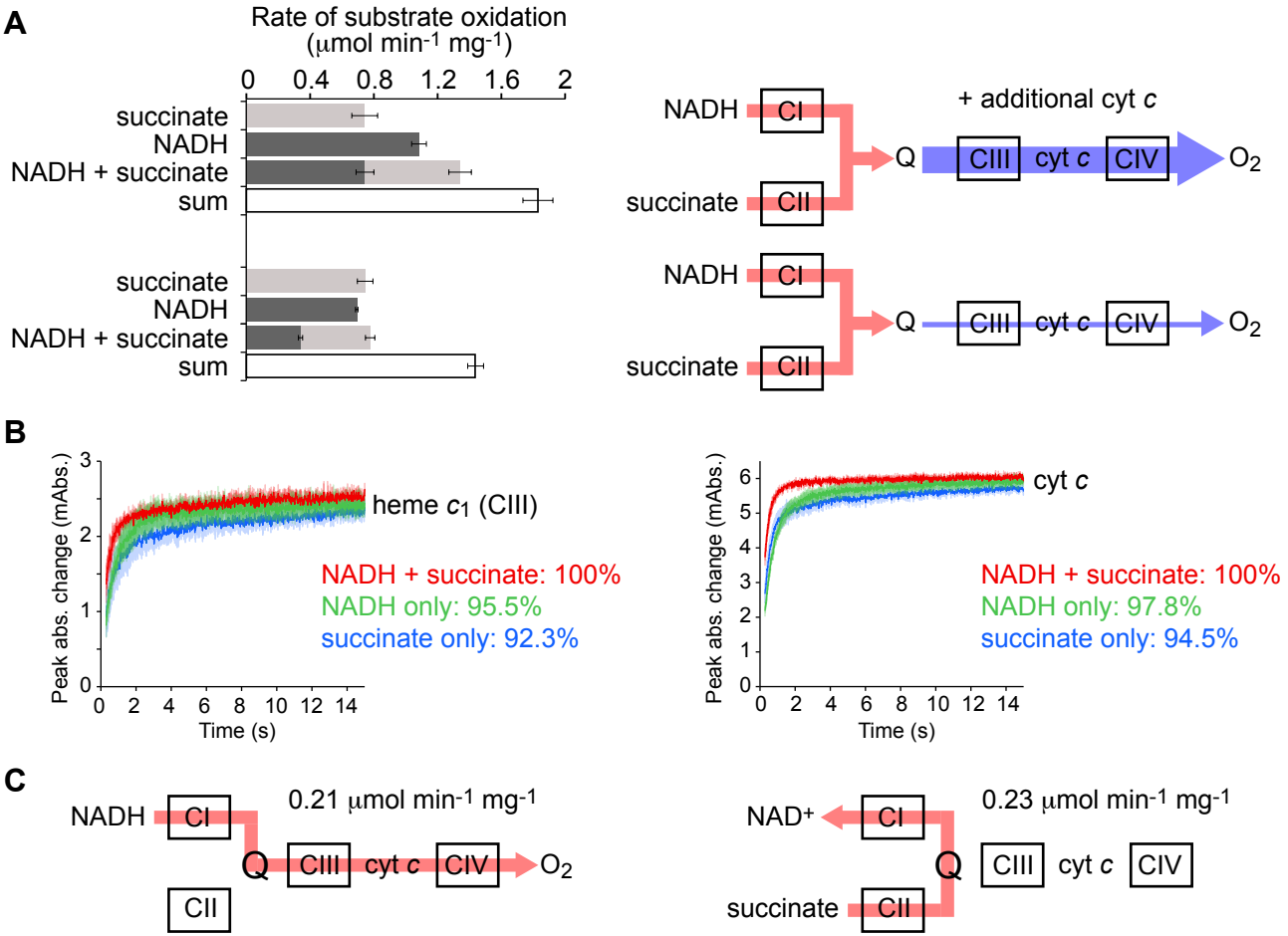
A
Rate of substrate oxidation
(μmol min-1 mg-1)
0
0.4
0.8
1.2
1.6
2
succinate
NADH
NADH + succinate
sum
succinate
NADH
NADH + succinate
sum
NADH
CI
succinate
CII
Q
CIII
cyt c
CIV
O2
+ additional cyt c
NADH
CI
succinate
CII
Q
CIII
cyt c
CIV
O2
B
Peak abs. change (mAbs.)
Time (s)
heme c1 (CIII)
NADH + succinate: 100%
NADH only: 95.5%
succinate only: 92.3%
Peak abs. change (mAbs.)
Time (s)
cyt c
NADH + succinate: 100%
NADH only: 97.8%
succinate only: 94.5%
C
NADH
CI
CII
Q
CIII
cyt c
CIV
O2
0.21 μmol min-1 mg-1
NAD+
CI
succinate
CII
Q
CIII
cyt c
CIV
0.23 μmol min-1 mg-1

Figure 5